J Clust Sci (2017) 28:3185–3192
DOI 10.1007/s10876-017-1285-y

ORIGINAL PAPER

Surface Oxidation of Supported, Size-Selected Silver Clusters

Tobias Lünskens[1] · Constantin A. Walenta[1] · Philipp Heister[1] · Aras Kartouzian[1] · Ueli Heiz[1]

Received: 4 April 2017 / Published online: 18 August 2017

Abstract We use surface second harmonic generation spectroscopy (s-SHG) to study the oxidation of supported, size-selected silver clusters under ultra-high vacuum conditions. The oxidation reaction of small silver clusters between Ag_9 and Ag_{55} is monitored by means of their localized surface plasmon resonance. We observe a rapid decline of the SH-intensity, as soon as cluster samples are exposed to an oxygen partial pressure of 5×10^{-6} mbar, which is attributed to the formation of silver–oxygen-bonds. The evolution of the SH-intensity under exposure to oxygen shows a double-exponential character for all investigated cluster sizes. Since the oxidation of single crystalline silver surfaces follow single-exponential Langmuir-kinetics, the two independent pathways of SH-intensity loss are attributed to a surface- and an interface-oxidation of supported clusters, respectiveley. For small cluster sizes, a complete loss of the SH intensity is obtained, which suggests the complete oxidation of the clusters. For larger clusters a plasmonic resonance is still observed after oxidation, indicating a residual free-electron density.

Keywords Supported silver clusters · Size selected clusters · Oxidation · Second harmonic generation spectroscopy

This work has been supported by the BMBF through the project IC4, the European Research Council through an Advanced Research Grant (246645-ASC3), and the DFG through the Project (HE 3454/21-1).

Tobias Lünskens and Constantin A. Walenta have contributed equally to this work.

✉ Aras Kartouzian
aras.kartouzian@tum.de

[1] Chemistry Department and Catalysis Research Center, Technical University of Munich, Lichtenbergstr. 4, 85748 Garching, Germany

Introduction

Silver as bulk material shows only limited catalytic activity and this is also true for the atomic form. However, silver particles show catalytic activity in various oxidation reactions, among them the industrially relevant epoxidation of ethylene with a selectivity of 90% [1]. The mechanisms of the reaction and the selectivity are still current topics of research even on single crystalline surfaces [2–5]. For nanoparticles, a clear particle size-effect is observed for the epoxidation of ethylene or higher unsaturated hydrocarbons [6–8]. Also the charge state of nanoparticles is a powerful means to control the reaction in heterogeneous catalysis. Optical spectroscopy offers a non-destructive in-situ approach to study the electronic structure of such particles. Particularly surface second-harmonic generation (s-SHG) spectroscopy is a promising tool to investigate the electronic structure of supported silver nanoparticles and clusters. This method has also been applied for in-situ monitoring of the oxidation reaction in case of large colloidal silver nanoparticles (80 nm in diameter) [9]. In a bottom-up approach, we explore the interaction of oxygen with silica supported, size-selected silver clusters spectroscopically. Many methods have been applied both experimentally [10, 11] and theoretically [12, 13] to understand the interaction of silver clusters and particles with oxygen. As a first step toward understanding the oxidation reaction, we investigate the influence of oxygen on the electronic structure of supported silver clusters by monitoring their optical response

Materials and Methods

The ultra-high vacuum (UHV) apparatus [14] and the spectroscopic setup [15], as well as the data analysis [16] have been described previously. Briefly, a high-frequency laser-vaporization cluster source is used to generate silver clusters. The second harmonic of a pulsed Nd:YAG laser is focussed onto a rotating metal target. The produced metal vapor is cooled by collisions with He buffer gas. The formed mixture of neutral, positively and negatively charged clusters of different sizes is expanded into vacuum and the positively charged metal clusters are guided to a quadrupole mass filter (QMF), where a specific cluster-size is chosen with atomic precision. The cationic clusters of one size are then soft-landed onto silica substrates (BK7), where they are neutralized by means of low-energy thermal electrons emitted from a hot filament. The following s-SHG measurements take place under UHV conditions (base pressure of 2×10^{-10} mbar) to discard any contamination of the samples. Cluster coverages do not exceed 3×10^{12} clusters per cm^2 to avoid agglomeration of size selected clusters as well as local field effects (this coverage corresponds to a mean cluster-cluster distance of $\approx$2 nm) [17]. S-SHG measurements are done in transmission and the samples are placed in Brewster's angle into the p-polarized (polarization parallel to the surface normal) laser beam to minimize reflections at the substrate surface. The fundamental of the pulsed laser beam (3 ps, $\approx$1 mJ/puls) is focussed onto the cluster sample and the generated second harmonic

light is detected by means of a photomultipliertube. It should be noted that the generation of second harmonic light is enhanced, if either the first harmonic or the generated second harmonic is in resonance with the system. All samples has been measured with the second harmonic in resonance to keep the input of energy into the system as low as possible. Prior to oxidation of silver clusters a complete s-SHG spectrum is measured in order to determine the size-depedent position of the plasmon resonance for each individual cluster size [17–19]. Subsequently after measuring a complete s-SHG spectrum, oxygen is dosed with a back pressure of 5×10^{-6} mbar on the sample with a temperature of ≈273 K and the oxidation process is monitored on-line at the maximum intensity of the plasmon resonance-peak by measuring the intensity of the SHG signal over time. This measuring procedure is applied for all individual samples of different cluster sizes.

Results and Discussion

Figure 1 shows a typical s-SHG spectrum of size-selected Ag_{35} clusters on a silica substrate. It should be noted that the strong oscillation of the data points is no signal noise, but is caused by interferences between the SHG contributions from the two surfaces of the substrate [16]. The onset of the interference pattern is located at ≈300 nm, coinciding with the absorption edge of the used glass substrates. In addition to the measured data points a lorentzian fit is depicted. It has been shown, that the peak in the s-SHG spectrum can be assigned to the localized surface plasmon resonance (LSPR) of the free 5*s*-electrons in silver clusters [20]. In good

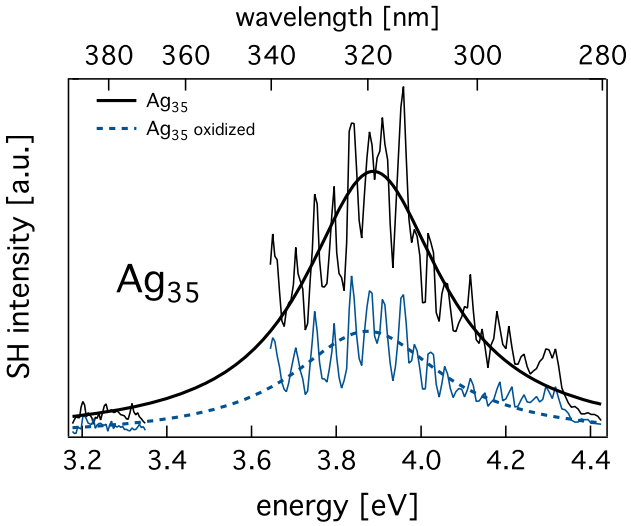

Fig. 1 s-SHG spectra of silica supported Ag_{35} clusters before and after exposure to oxygen. The measured data are fitted with lorentzians. The *black solid line* shows the sample before oxidation. The *dashed blue line* shows the spectrum on the same spot on the sample after oxidaiton with molecular oxygen (Color figure online)

agreement with literature a LSPR of ≈3.9 eV is observed for supported Ag_{35} clusters [17, 21, 22]. The dashed blue line in Fig. 1 corresponds to the spectrum of the same sample after oxidation with molecular oxygen. The signal is damped to about 60% of the original intensity of the clean sample, which can be assigned to a reduced polarizability of the free conduction electrons [23, 24]. It is known, that molecular oxygen dissociates on silver and forms strongly bound atomic oxygen species, localizing conduction electrons in silver–oxygen-bonds [25]. However, the plasmonic resonance is neither shifted nor broadened (before oxidation the plasmon resonance peak is located at 3.89 ± 0.1 eV with a FWHM of 0.39 ± 0.1 eV; after oxidation the peak is located at 3.87 ± 0.1 eV with a FWHM of 0.43 ± 0.1 eV). We think that this counter intuitive observation can be explained by the used spectroscopic technique, which is addressed in the conclusion. Assuming a similar behavior for all measured cluster-sizes the evolution of the signal intensity under exposure to oxygen can be measured at a single wavelength, which is shown in Fig. 2 for Ag_{35}. As soon as an oxygen partial pressure of 5×10^{-6} mbar is applied to the samples, the SH intensity drops in a double-exponential manner indicating the presence of a rapid and a slow decline (Fig. 2) for all measured cluster sizes. The rapid decline at the beginning possesses a time constant in the range of 40 s (a dosage of 40 s with an applied pressure of 5×10^{-6} mbar corresponds to a dosage of ≈150 Langmuir), whereas the slow decline possesses a time constant in the range of 1000 s (≈3800 L). Because no decrease of the SH-intensity is observed without dosing oxygen, both independent pathways of SH-intensity loss can be assigned to

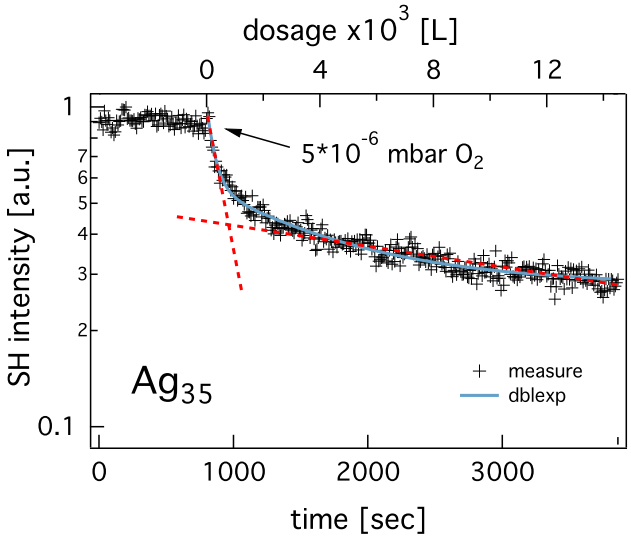

Fig. 2 SH intensity of silica supported Ag_{35} clusters measured at an energy of 3.9 eV (which is the resonance peak of this specific cluster size) during exposure to an oxygen partial pressure of 5×10^{-6} mbar. The decay of SH intensity follows a double-exponential character. Note that the SH intensity is depicted on a logarithmic scale. The *two red dashed lines* are indicating the two oxidation regimes. The dosage in Langmuir is calculated from the duration of exposure and the applied pressure of 5×10^{-6} mbar (Color figure online)

reaction with oxygen. As shown in the earlier works, photodegradation of the cluster-samples can be excluded under the applied experimental conditions [20].

Other groups have used SHG-spectroscopy to monitor the oxidation of single crystalline silver surfaces in UHV as well as colloidal silver nanoparticles [9, 26]. In contrast to the results for supported silver nanoparticles presented in this work, a monotonic decrease of SH-intensity following a single-exponential Langmuir kinetic was observed. To explain the two independent pathways of SH-intensity loss, the substrate has to be taken into account. If each surface atom is assumed to be equivalent, supported clusters can be characterized by two different adsorption sites, surface atoms, which are located away from the support-surface can be distinguished from interfacial atoms at the cluster perimeter. For oxide supported palladium and silver clusters it was found that the dissociative adsorption of oxygen is energetically favored at interfacial sites compared to surface atoms away from the substrate [27, 28]. It should be noted that oxygen might not only influence supported silver clusters directly. As seen in another study by Mao et al., the oxygen environment influences also the electronic structure of the support [29], which is, however, impossible to disentangle with s-SHG spectroscopy. Considering a similar scenario for silica supported silver clusters, the rapid drop in intensity at the beginning can be attributed to a dissociative adsorption at interfacial sites, whereas the slow decrease of SH-intensity can be attributed to an oxidation of surface atoms away from the support. However, it cannot be entirely excluded that the fast SH-intensity drop observed in this work is due to a gasphase oxidation of surface-sites, whereas the slow SH-intensity decrease is caused by a substrate mediated oxidation of interfacial sites. Adsorption of oxygen on Ag(100), which does not exhibit interfacial adsorption sites, shows a time constant equivalent to ≈100 L, which is very similar to the fast intensity decline observed in this work (≈150 L) [30]. It should be noted that the properties of small particles may differ from extended surfaces significantly and, therefore, this comparison should be handled with care. Whatever the order, supported silver clusters undergo a complete surface oxidation, whereas the SH-intensity after oxidation can be assigned to the resonance of the remaining free electron density.

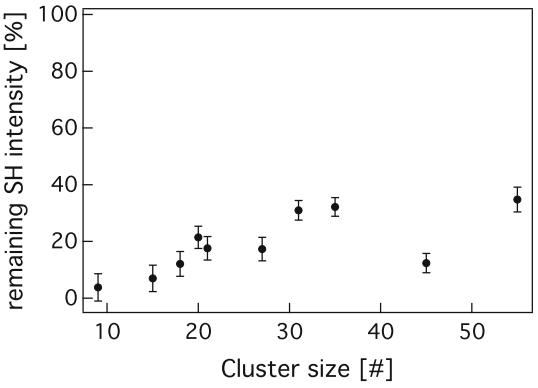

Fig. 3 Remaining SH intensity of size-selected silica supported silver clusters after exposure to an oxygen partial pressure of 5×10^{-6} mbar

In Fig. 3 the remaining SH-intensity after oxidation is shown for cluster sizes between Ag_9 and Ag_{55}. A clear trend of the signal loss with the cluster size is observed. Very small clusters like Ag_9 loose the full SHG signal under exposure to oxygen, suggesting that every atom is a surface- or interface-atom. It should be noted, that even for Ag_9 two independent pathways for the decrease in SH-intensity are observed, indicating a three dimensional cluster, in agreement with previous observations [17]. For larger cluster sizes, some residual SH-intensity is measured after oxidation, which is attributed to remaining free electron density. It can be suggested, that core atoms of bigger silver clusters are not oxidized under the experimental conditions used here. The deviations from the general trend, for example observed in the case of Ag_{45}, might be caused by specific cluster geometries, which, however, can not be elucidated with SHG-spectroscopy solely.

Conclusion

In this study, we demonstrate that supported, size-selected silver clusters interact with molecular oxygen at room temperatures. An SH-intensity loss of the LSPR is observed for the interaction with O_2, which is attributed to a reduced polarizability of initially free conduction electrons localized in silver–oxygen bonds. The evolution of the LSPR intensity under oxygen exposure possesses a double-exponential character, which is attributed to a surface- and an interface-oxidation of supported clusters. For small cluster sizes, a complete loss of the SH intensity is obtained, which suggests the complete oxidation of the clusters, where all atoms in the cluster are either surface or interface atoms. For larger clusters a plasmonic resonance is still observed after oxidation, indicating a residual free-electron density. We can show, that all silver cluster sizes investigated in this work interact with oxygen and build localized bonds, that can form an active intermediate species for oxidation catalysis experiments.

Interestingly, the plasmon resonance peak in the s-SHG spectrum of the oxidized sample is neither shifted nor broadened in comparison to the clean sample. This is in contrast to varios studies on LSPR of coinage metal nanoparticles, which show a shift and broadening of the LSPR due to change in the electron density as well as dielectric constant of the surrounding medium [31, 32]. For silver nanoparticles it has been shown that the effective dielectric constant of the nanoparticles increase with surface oxidation, resulting in a redshift of the plasmon resonance [33]. In the case of nonlinear optical techniques, like SHG, similar effects are expected [34, 35]. A possible explanation could be, that even in the case of ultra small silver clusters the generation of second harmonic light is restricted to surface atoms solely, similar to extended surfaces [26, 36]. Further studies are needed in order to fully understand the behavior of the SHG-signal corresponding to the LSPR of small silver clusters.

References

1. J. W. Niemantsverdriet and I. Chorkendorff *Concepts of Modern Catalysis and Kinetics*, 2nd ed (Wiley, New York, 2007).
2. P. Christopher and S. Linic (2008). *J. Am. Chem. Soc*. **130**, (34), 11264.
3. P. Christopher, H. Xin and S. Linic (2011). *Nat. Chem*. **3**, (6), 467.
4. S. Böcklein, S. Günther and J. Wintterlin (2013). *Angew. Chem. Int. Ed*. **52**, (21), 5518.
5. S. Böcklein, S. Günther, R. Reichelt, R. Wyrwich, M. Joas, C. Hettstedt, M. Ehrensperger, J. Sicklinger and J. Wintterlin (2013). *J. Catal*. **299**, 129.
6. S. Vajda, S. Lee, K. Sell, I. Barke, A. Kleibert, V. von Oeynhausen, K. H. Meiwes-Broer, A. F. Rodriguez, J. W. Elam, M. M. Pellin, B. Lee, S. Seifert and R. E. Winans (2009). *J. Chem. Phys*. **131**, (12), 121104.
7. L. M. Molina, S. Lee, K. Sell, G. Barcaro, A. Fortunelli, B. Lee, S. Seifert, R. E. Winans, J. W. Elam, M. J. Pellin, I. Barke, V. von Oeynhausen, Y. Lei, R. J. Meyer, J. A. Alonso, A. F. Rodríguez, A. Kleibert, S. Giorgio, C. R. Henry, K. H. Meiwes-Broer and S. Vajda (2011). *Catal. Today* **160**, (1), 116.
8. Y. Lei, F. Mehmood, S. Lee, J. Greeley, B. Lee, S. Seifert, R. E. Winans, J. W. Elam, R. J. Meyer, P. C. Redfern, D. Teschner, R. Schlögl, M. J. Pellin, L. A. Curtiss and S. Vajda (2010). *Science* **328**, (5975), 224.
9. W. Gan, G. Gonella, M. Zhang and H. L. Dai (2011). *J. Chem. Phys*. **134**, (4), 041104.
10. M. Schmidt, A. Masson and C. Bréchignac (2003). *Phys. Rev. Lett*. **91**, 243401.
11. O. S. Ivanova and F. P. Zamborini (2010). *J. Am. Chem. Soc*. **132**, (1), 70.
12. E. A. Carter and W. A. Goddard (1989). *Surf. Sci*. **209**, (1), 243.
13. S. Klacar, A. Hellman, I. Panas and H. Grönbeck (2010). *J. Phys. Chem. C* **114**, (29), 12610.
14. A. Kartouzian, M. Thaemer, T. Soini, J. Peter, P. Pitschi, S. Gilb and U. Heiz (2008). *J. Appl. Phys*. **104**, (12), 124313/1.
15. M. Thaemer, A. Kartouzian, P. Heister, S. Gerlach, M. Tschurl, U. Boesl and U. Heiz (2012). *J. Phys. Chem. C* **116**, (15), 8642.
16. A. Kartouzian, P. Heister, M. Thämer, S. Gerlach and U. Heiz (2013). *J. Opt. Soc. Am. B* **30**, (3), 541.
17. T. Lünskens, P. Heister, M. Thämer, C. A. Walenta, A. Kartouzian and U. Heiz (2015). *Phys. Chem. Chem. Phys*. **17**, (27), 17541.
18. K. P. Charle, W. Schulze and B. Winter (1989). *Zeitschrift für Physik D Atoms, Molecules and Clusters* **12**, (1–4), 471.
19. E. Loginov, L. F. Gomez, N. Chiang, A. Halder, N. Guggemos, V. V. Kresin and A. F. Vilesov (2011). *Phys. Rev. Lett*. **106**, 233401. doi:10.1103/PhysRevLett.106.233401.
20. M. Thämer, A. Kartouzian, P. Heister, T. Lünskens, S. Gerlach and U. Heiz (2014). *Small* **10**, 2340–2344.
21. H. Haberland (2013). *Nature* **494**, E1–E2.
22. R. Lazzari, J. Jupille, R. Cavallotti and I. Simonsen (2014). *J. Phys. Chem. C***118**, (13), 7032.
23. N. Bloembergen, R. K. Chang, S. S. Jha and C. H. Lee (1968). *Phys. Rev*. **174**, 813.
24. V. R. Thierry Verbiest and K. Clays *Second-Order Momlinear Optical Characterization Techniques: An Introduction* (CRC Press, New York, 2009).
25. B. A. Sexton and R. J. Madix (1980). *Chem. Phys. Lett*. **76**, (2), 294.
26. D. Heskett, L. Urbach, K. Song, E. Plummer and H. Dai (1988). *Surf. Sci*. **197**, (1–2), 225.
27. B. Yoon, U. Landman, V. Habibpour, C. Harding, S. Kunz, U. Heiz, M. Moseler and M. Walter (2012). *J. Phys. Chem. C***116**, (17), 9594.
28. L. Cheng, C. Yin, F. Mehmood, B. Liu, J. Greeley, S. Lee, B. Lee, S. Seifert, R. E. Winans, D. Teschner, R. Schlögl, S. Vajda and L. A. Curtiss (2014). *ACS Catal*. **4**, (1), 32.
29. B. H. Mao, R. Chang, L. Shi, Q. Q. Zhuo, S. Rani, X. S. Liu, E. C. Tyo, S. Vajda, S. D. Wang and Z. Liu (2014). *Phys. Chem. Chem. Phys*. **16**, 26645.
30. D. Heskett, L. Urbach, K. Song, E. Plummer and H. Dai (1988). *Surf. Sci*. **197**, (1), 225.
31. J. J. Mock, D. R. Smith and S. Schultz (2003). *Nano Lett*. **3**, (4), 485.
32. C. Novo, A. M. Funston, A. K. Gooding and P. Mulvaney (2009). *J. Am. Chem. Soc*. **131**, (41), 14664.
33. J. Butet, I. Russier-Antoine, C. Jonin, N. Lascoux, E. Benichou and P. F. Brevet (2013). *J. Phys. Chem. C* **117**, (2), 1172.

34. J. Butet, I. Russier-Antoine, C. Jonin, N. Lascoux, E. Benichou and P. F. Brevet (2012). *Nano Lett.* **12**, (3), 1697.
35. J. Butet, I. Russier-Antoine, C. Jonin, N. Lascoux, E. Benichou and P. F. Brevet (2013). *J. Phys. Chem. C* **117**, (2), 1172.
36. Y. R. Shen (1989). *Annu. Rev. Phys. Chem.* **40**, 327.